Journal of Structural Engineering & Applied Mechanics (2025) 8(4):348-361
DOI 10.31462/jseam.2025.04348361

RESEARCH ARTICLE

Numerical investigation of sinusoidally patterned thin-walled tubes with variable wall thickness under quasi-static axial loading

Hamdi Kuleyin[1*]

[1] Recep Tayyip Erdogan University, Department of Mechanical Engineering, Rize, Türkiye

Article History

Received 05 November 2025
Accepted 25 December 2025

Keywords

Thin-walled tubes
Energy absorption
Corrugation strategies
Crashworthiness
Axial compression
Finite element method

Abstract

Enhancing the crashworthiness and energy-absorption capacity of lightweight tubular structures is essential for improving safety while meeting modern demands for weight reduction in engineering applications. This study aims to investigate the effects of sinusoidal corrugation patterns with variable wall thickness on the crashworthiness behavior of circular thin-walled tubes. A validated 2D axisymmetric finite-element model was developed in LS-DYNA, and corrugated tube configurations were designed with one-sided (OS) and double-sided (DS) thickness variations, and their quasi-static compression responses were examined. The results revealed that corrugation geometry significantly enhances crashworthiness characteristics compared to a straight tube. The OS-2.75 configuration exhibited the most pronounced improvements, achieving increases of 31% in mean crushing force, 34.3% in total absorbed energy, and 13.5% in specific energy absorption (SEA). Meanwhile, the DS-2.75 model showed enhancements of up to 24% and 20% in mean crushing force and total energy absorption, respectively, with the DS-2.5 tube offering a favorable balance between mass reduction and improved performance. The findings demonstrate that corrugation-based thickness tailoring is a robust and efficient design strategy for improving the crashworthiness of thin-walled tubes. The presented approach offers valuable guidelines for the development of lightweight energy-absorbing components in automotive, aerospace, and protective engineering applications.

1. Introduction

Thin-walled tubes have been widely used as passive energy absorbers in many engineering applications, such as automotive, aerospace, and railways, for decades, thanks to their excellent energy-absorbing properties [1]. In recent years, growing attention has been directed toward the design of thin-walled tubes that simultaneously achieve lightweight characteristics and high energy absorption efficiency, driven by the interrelation among fuel efficiency, crashworthiness, structural weight reduction, and carbon emission concerns [2-4].

In this regard, many studies have focused on investigating various thin-walled tube configurations employing different materials, cross-sectional geometries, structural designs, and filler types in the tube gap [5-7]. Previous studies revealed that variations in cross-sectional design significantly affect the energy

* Corresponding author (hamdi.kuleyin@erdogan.edu.tr)
eISSN 2630-5763

absorption performance of thin-walled columns [8]. In the literature, various approaches, such as corrugated or grooved, and functionally graded cross-sectional geometries or thin-walled tube designs, have been investigated to optimize the crashworthiness performance of thin-walled structures and to achieve a stable energy absorption process in addition to the effect of cross-sectional types [9-11]. Especially, corrugation of the thin-walled tube approaches has attracted much attention because this approach can contribute to controlling the energy absorption, deformation sequence, and fluctuation in crushing force. For example, Singace and El-Sobky [12] experimentally investigated the effects of corrugation approach on the axial crushing behavior of circular thin-walled tubes, such as energy absorption capacity and deformation sequence. Their results showed that the corrugations improved the load-displacement curve of the tubes more smoothly and reduced sudden load fluctuations during the deformation. Eyvazian et al. [13] examined the deformation modes and energy absorption characteristics of aluminum thin-walled tubes with experimental tests. The results showed that the corrugated tubes offer controllable deformation modes, and energy absorption behavior depends on the number of corrugations and amplitude. Wu et al. [14] focused on experimental, numerical, and analytical investigation of corrugated thin-walled tubes with sinusoidal patterns. It can be presented that the corrugation strategies led to a considerable decrease in initial peak force and a significant increase in the load-carrying capability. Similarly, Kılıçaslan [15] examined the effects of sinusoidal pattern on the crashworthiness performance of the thin-walled tube. It can be reported that sinusoidal patterns cause a significant improvement in crushing force efficiency. In addition to experimental studies, Chen and Ozaki [16] numerically investigated the axial crushing behavior of circular corrugated tubes using the finite element method. Their results revealed that corrugation has a significant influence on the deformation behavior and force-displacement characteristics, deformation behavior leading to distinct axisymmetric and asymmetric crushing modes characterized by different load–load-displacement responses. Numerical results showed that the corrugated tubes exhibit lower initial peak force, a more stable deformation mode, and uniform crushing force. Moreover, Hao et al. [17] theoretically discussed the prediction of the deformation and energy absorption properties of a sinusoidal patterned tube under axial loading. Also, the better crush force efficiency and specific energy absorption properties were achieved with a thin-walled tube of corrugated surfaces reported from earlier studies [18]. Koloushani et al. [19] investigated the effects of design parameters of longitudinal corrugated tubes, such as amplitude, number of corrugations, on crashworthiness performance and deformation modes with numerical modeling. Also, they optimized corrugation patterns to desired performance outputs, such as reducing maximum crush force and increasing the specific energy absorption compared to straight tubes. Alkhatib et al. [20] fabricated the longitudinally sinusoidal patterned thin-walled tubes with an additive manufacturing technique. Their experimental results showed that a significant reduction was achieved in the initial peak force while the crush force efficiency increased considerably. Moreover, considering the recent progress in additive manufacturing techniques, it has been stated that corrugated structures enable effective design optimization processes aimed at reaching the targeted structural performance [9]. Although numerous studies in the literature have investigated various enhancement strategies, such as corrugated, grooved, and functionally graded thickness configurations, for improving the crashworthiness performance of thin-walled tubes, a detailed investigation of how sinusoidal corrugation combined with variable wall-thickness transitions influences crashworthiness performance is still lacking [9, 21]. For instance, corrugation strategies have a critical role in the localized stiffening, deformation stability, and fold initiation, controlling reported in literature [10]. The studies discussed have revealed that corrugation of the thin-walled tube surface promotes more stable deformation modes and crush force responses. As a result of stable crushing force behavior, the energy absorption capacity of the tubular structure achieved an excellent level. Previous research in the literature has extensively examined the effects of parameters such as cross-sectional geometry, number of corrugations, wavelength, and material type on the behavior of sinusoidal corrugated tubes through experimental, numerical, and theoretical approaches. However, no parametric study has been reported in the literature that examines the effects of wall-thickness transitions in corrugated tubes on key crashworthiness performance parameters such as absorbed energy, specific energy absorption capacity, and crushing force response of circular thin-walled structures.

The present study aims to conduct a systematic investigation of thin-walled tubes that concurrently employ sinusoidal corrugation and regionally increased wall thickness, a configuration not previously examined in the literature with respect to deformation modes and key crashworthiness indices such as peak load, mean crushing force, SEA, and CFE. The mechanical relevance of variable wall thickness within corrugated regions is grounded in deformation theories. Local thickening promotes higher bending stiffness, shifts plastic hinge formation toward thick regions, and causes overlapping deformation lobes during crushing mechanisms known to increase fold resistance and stabilize the deformation sequence [9, 22]. As a result, tailoring the variable wall-thickness within corrugated patterns is expected to generate substantially higher mean crushing force and improved energy-absorption capacity compared with uniform-thickness corrugated tubes. In this study, numerical analysis is conducted on cylindrical thin-walled tubes with one- and double-sided sinusoidally corrugations that consist of variable wall thickness under quasi-static compression loading. The energy absorption characteristics of the corrugated (one- and double-sided at variable wall thickness) and straight tubes were compared via crushing performance parameters such as absorbed energy, specific energy absorption, and crush force efficiency.

2. Materials and methods

2.1. Geometry of thin-walled tubes and material properties

To investigate the influence of variable wall thickness on the mechanical behavior of corrugated circular thin-walled tubes, specimens were configured with L/D and r/t ratios of 3 and 12.5, respectively. Accordingly, the reference tubes possessed a wall thickness of 2 mm, a diameter of 50 mm, and a total length of 150 mm. On this basic tube geometry, sinusoidal corrugation patterns were applied to generate regional thickness variations of 2.25, 2.5, and 2.75 mm, respectively.

The one-sided and double-sided corrugated tube geometries were constructed parametrically using a periodic half-sine formulation to represent wall-thickness transitions along the tube axis. Let x denote the axial coordinate measured from the bottom end of the corrugation patterns, such that $0 < x < l$. Each corrugation occupies an axial length l, which differs for each configuration. To ensure smooth and continuous geometric variation, a half-sine wave was repeated periodically along the entire tube length. The periodic function was constructed using the absolute sine term, which avoids discontinuities at the corrugation boundaries. The nominal tube thickness was 2.0 mm, and the thickness in the corrugated regions (t_c) gradually increased to 2.25 mm, 2.5 mm, and 2.75 mm for different corrugated tube designs, respectively. Thus, the local thickness amplitude is

$$\Delta t = t_c - t \tag{1}$$

The thickness variation along the tube was defined by:

$$t(x) = t + \Delta t \left|\sin\left(\frac{\pi x}{l}\right)\right| \tag{2}$$

With this formulation, the thickness was obtained as t = 2 mm at every corrugation boundary (x = 0 and l), and the thickness obtained as t_c = 2.25 mm, 2.5 mm, and 2.75 mm at the midpoint of the corrugation (x = l/2) for different thickness variations, respectively.

Table 1. Sample codes of tube designs and geometric dimensions

Tube design	Sample code	Geometric dimensions (mm)					Number of corrugations
		t	t_c	l	r	r_c	
Straight	S		2	-	-	-	-
One Side Corrugated Tube (2.25 mm)	OS-2.25		2.25	2.5	1	1.25	60
One Side Corrugated Tube (2.5 mm)	OS-2.5		2.5	3.5	1	1.5	43
One Side Corrugated Tube (2.75 mm)	OS-2.75	2	2.75	4.25	1	1.75	35
Double Side Corrugated Tube (2.25 mm)	DS-2.25		2.25	2.5	1.9	2.4	60
Double Side Corrugated Tube (2.5 mm)	DS-2.5		2.5	3.5	1.8	2.6	43
Double Side Corrugated Tube (2.75 mm)	DS-2.75		2.75	4.25	1.9	2.9	35

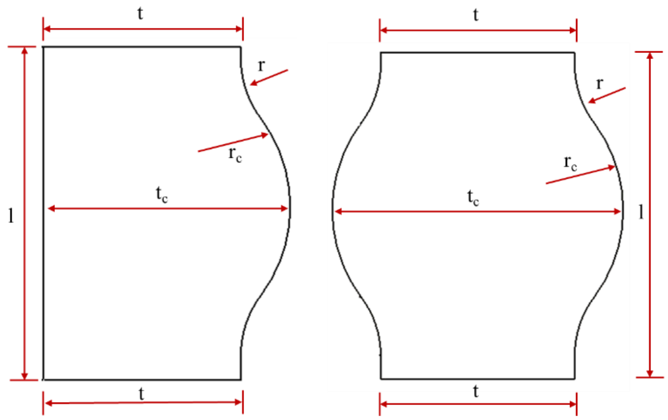

(a) (b)

Fig. 1. The geometric design and dimensions of corrugated thin-walled tubes with variable tube-wall thickness; a) one side corrugated and b) double side corrugated

Similar to the thickness variation along the tube wall, the radius transitions along the tube wall are defined by

$$\Delta r = r_c - r \tag{3}$$

$$r(x) = r + \Delta r \left|\sin\left(\frac{\pi x}{l}\right)\right| \tag{4}$$

From this formulation, the radius obtained is r and r_c at the start/end of corrugation and at the midpoint of the corrugation, respectively. With this parametric formulation allowed each tube configuration to be constructed with consistent geometric smoothness, precise control of the corrugation amplitude and wavelength, and a physically meaningful continuous wall-thickness transition, enabling accurate assessment of the influence of variable wall-thickness corrugation on the crashworthiness performance of circular thin-walled tubes. Accordingly, thin-walled circular tubes with different wall-thickness transition regions were designed using sinusoidal geometry–based corrugation patterns for both one-sided and double-sided configurations. The geometric dimensions corresponding to a representative corrugation pattern, which yields wall-thickness regions of 2.25 mm, 2.5 mm, and 2.75 mm, are summarized in Table 1.

Fig. 1 presents the unit cross-sectional geometries for the one-sided and double-sided corrugated tube configurations, along with the corresponding dimensional parameters. In addition, the number of corrugations along the 150 mm tube length for each configuration is summarized in Table 1. As can be observed from the unit cross-section illustrated in Fig. 1, the sinusoidal patterns were designed to produce variable wall thickness along the tube axis, rather than maintaining a constant thickness. To facilitate a clear distinction between the numerical models developed using the aforementioned tube geometries, the model labels and abbreviations employed throughout the numerical analyses are also provided in Table 1.

2.2. Finite element modeling

The numerical models were developed using the ANSYS-LS DYNA package program the investigate the effects of sinusoidal corrugation patterns with variable thickness on the crush force responses, energy absorption capacity, and evaluate the efficiency of crush performance. For this aim, in this study, finite element modeling methodology was used to create the axisymmetric numerical models for straight and corrugated circular thin-walled tubes. The material and mechanical properties of the tubes that were used in numerical models were summarized in Table 2.

The schematic illustration of the numerical model is given in Fig. 2a. This model consists of three main components: a thin-walled tube, an upper moving plate, and a fixed plate. The thin-walled tube, upper moving plate, and fixed plate were modeled using axially symmetric volume-weighted elements. For modeling the material and mechanical properties of tube MAT-PIECEWISE-LINEAR-ISOTROPIC-PLASTICITY. Also, MAT-20-RIGID material cards were used for modeling both the upper moving plate and fixed plate; also, the material and mechanical properties of the plates are given in Table 2. Mechanical properties of the aluminum thin-walled tube modeled with the true stress-true strain curve of tube material (aluminum 6063-T5 [23]) given in Fig. 2b.

Table 2. Material and mechanical properties of thin-walled tubes and rigid plates [23]

Material	P (g/cm^3)	Modulus of elasticity (GPa)	Yield strength (MPa)	Ultimate tensile strength (MPa)	ν
Tube	2700	68.2	180	206	0.3
Rigid Plates	7800	210	-	-	0.3

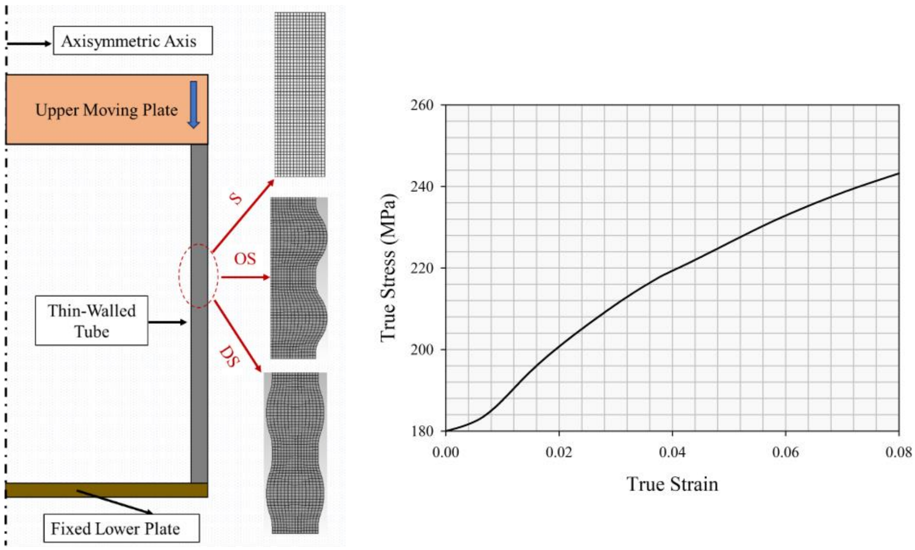

(a) (b)

Fig. 2. (a) The schematic illustration of the 2D axially symmetric numerical models, and (b) true stress-strain curve of tube material [23]

The contact interaction between the tube and the upper loading plate was modeled using the 2D Automatic Surface-to-Surface contact algorithm, while the 2D Automatic Single-Surface contact algorithm was employed to represent the self-contact behavior of the tube during deformation. The axial load response was obtained by monitoring the force evolution at the nodes located at the fixed and impact ends of the tube, as well as by tracking the contact forces developed between the tube and the rigid plate. For this purpose, the RCFORC control cards were utilized. For validation of the finite element model, the force-displacement curves and their energy absorption capacity obtained from the compression test of a circular thin-walled tube carried out by Acar et al. [24] were used. The experimental and numerical results reported in literature [24], together with the force–displacement curves and total absorbed energy values obtained from the 3D shell model in LS-DYNA and the 2D axisymmetric model developed in this study, were comparatively evaluated to verify the model validation. Through this comparison, the consistency between the numerical predictions and experimental observations was demonstrated, thereby establishing the validity of the proposed modeling approach.

2.3. Crushing performance parameters

Mechanical responses of straight and corrugated circular thin-walled tubes with the effects of variable wall thickness were examined on crushing performance parameters such as absorbed total energy (EA), specific energy absorption (SEA), initial peak force (IPF), mean crushing force (MCF), and crushing force efficiency (CFE). The crushing performance parameters are usually used to determine the energy absorption performance of the structure given below [25].

The absorbed total energy (EA) of a thin-walled tube can be described by integrating the crush force corresponding to the displacement as follows [26]:

$$\mathrm{EA} = \int_0^s P(s)ds \tag{5}$$

where s denotes the crushing deformation distance and P the crushing force during the deformation. Also, another important crash performance parameter SEA can be determined as energy absorption completed per unit mass [25, 27].

$$\mathrm{SEA} = \frac{\mathrm{EA}}{m} \tag{6}$$

where m is the mass of the thin-walled tube. Mean crushing force (MCF) is the average of the crushing force during the deformation, expressed as the ratio of energy absorption to deformation distance. The parameter of crushing force efficiency (CFE) is expressed as the ratio of the MCF to the IPF in the following expression [28]:

$$\mathrm{MCF} = \frac{\mathrm{EA}}{s} \tag{7}$$

$$\mathrm{CFE} = \frac{\mathrm{MCF}}{\mathrm{IPF}} \tag{8}$$

3. Results and discussion

3.1. Validation of the numerical model

For the validation of the 2D axisymmetric model employed in this study, the experimental compression test data and numerical simulation results reported by Acar et al. [24] for circular thin-walled aluminum tubes were utilized. Also, the effect of mesh size on the numerical force-displacement curves and deformation modes, and mesh convergence analysis, was completed for numerical model verification. For the mesh convergence analysis, thin-walled tube models with element sizes of 0.25 mm, 0.125 mm, and 0.0625 mm were created, and the convergence assessment was conducted based on the force–displacement responses and numerical solution times obtained from the corresponding 2D model results. The force–displacement curves obtained from numerical models with different mesh sizes, together with the corresponding curves extracted from the experimental reference study, as well as the absorbed energy values calculated from these curves, were used to perform the mesh convergence analysis.

Fig. 3 presents a comparative illustration of the force–displacement curves and absorbed energy–displacement curves for different mesh sizes. To evaluate the influence of mesh density on the numerical results, force–displacement and energy absorption–displacement responses obtained from three different mesh sizes (0.25 mm, 0.125 mm, and 0.0625 mm) were examined. As shown in Fig. 3, reducing the element size does not lead to appreciable variations in the peak crushing forces and in the total absorbed energy. The overall crushing force responses and energy absorption characteristics remain largely mesh-independent. In addition to the mechanical response, the computational efficiency of each model was assessed. The solution times for the 0.25 mm, 0.125 mm, and 0.0625 mm models were recorded as 3302 s, 20,045 s, and 238,406 s, respectively, indicating that mesh refinement imposes a substantial increase in computational cost. Notably, the jump from 0.125 mm to 0.0625 mm results in more than an order-of-magnitude increase in solution time without providing a commensurate improvement in the predicted structural response. Taking into account the negligible variation in crushing force and energy absorption with mesh refinement, the drastic rise in computational time at smaller mesh sizes, and the fact that a 0.25 mm mesh would be insufficiently refined in the corrugation transition regions, an element size of 0.125 mm was selected as the optimal mesh resolution for all subsequent numerical analyses.

To validate the numerical model, experimental and numerical crushing force–displacement responses obtained from literature [24] over a 100 mm deformation distance were taken into consideration and compared with the results of the 2D axisymmetric model developed herein. In addition, the experimental and numerical deformation images were compared with the deformation patterns obtained by the present 2D axisymmetric model to further assess its accuracy. The crushing force-displacement curves, absorbed energy-displacement curves, and deformed shape images of the thin-walled tubes are given in Fig. 4. As shown in Fig. 4a, examination of the force–displacement curves indicates that the initial peak crushing forces for the experimental test, the 3D model, and the 2D model were obtained as 68.5 kN, 66.8 kN, and 64.2 kN, respectively. This comparison demonstrates that the initial peak force predicted by the 2D axisymmetric model used in this study is in strong agreement with the numerical results reported in literature [24]. Furthermore, the absorbed energy values for the experimental, 3D numerical, and 2D axisymmetric models were determined as 4.04 kJ, 4.29 kJ, and 4.29 kJ, respectively. These results confirm that the total energy absorption capacity predicted by the present 2D model is consistent with both the experimental findings and the numerical results from the previous study. In addition to the numerical correlations, the deformed images of the thin-walled tube obtained from the experimental test, the 3D model, and the 2D axisymmetric model are presented in Fig. 4c. As observed, the progressive folding sequence and overall deformation modes obtained by the 2D model show strong similarity to those reported in the previous work [24].

3.2. One side corrugated tubes

This section presents the effects of one-sided corrugation with variable thickness on the quasi-static compression behavior of a thin-walled tube. Figs. 5a and 5b illustrates the comparison of the crushing force-displacement and mean crushing force-displacement curves obtained from the straight, OS-2.25, OS-2.5, and

OS-2.75 tube sections, respectively. Also, obtained initial peak crushing force and mean crushing force values are given in Table 3.

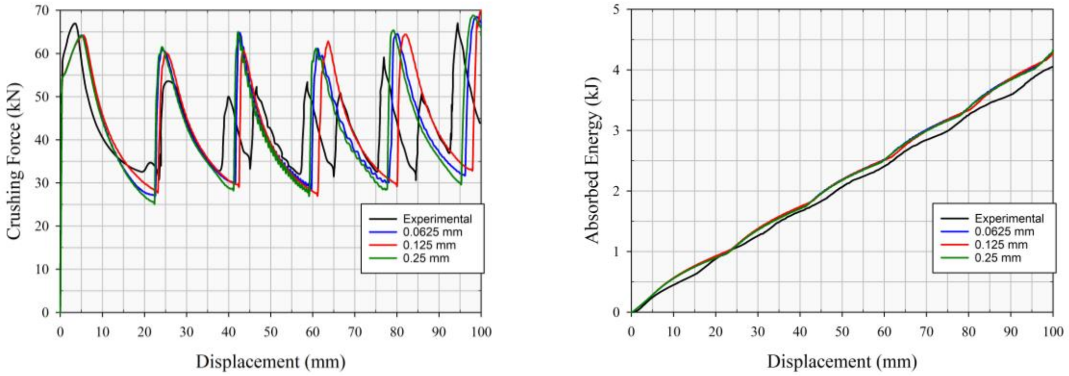

(a) (b)

Fig. 3. Effect of mesh size on (a) force–displacement and (b) absorbed energy–displacement responses of the 2D axisymmetric model

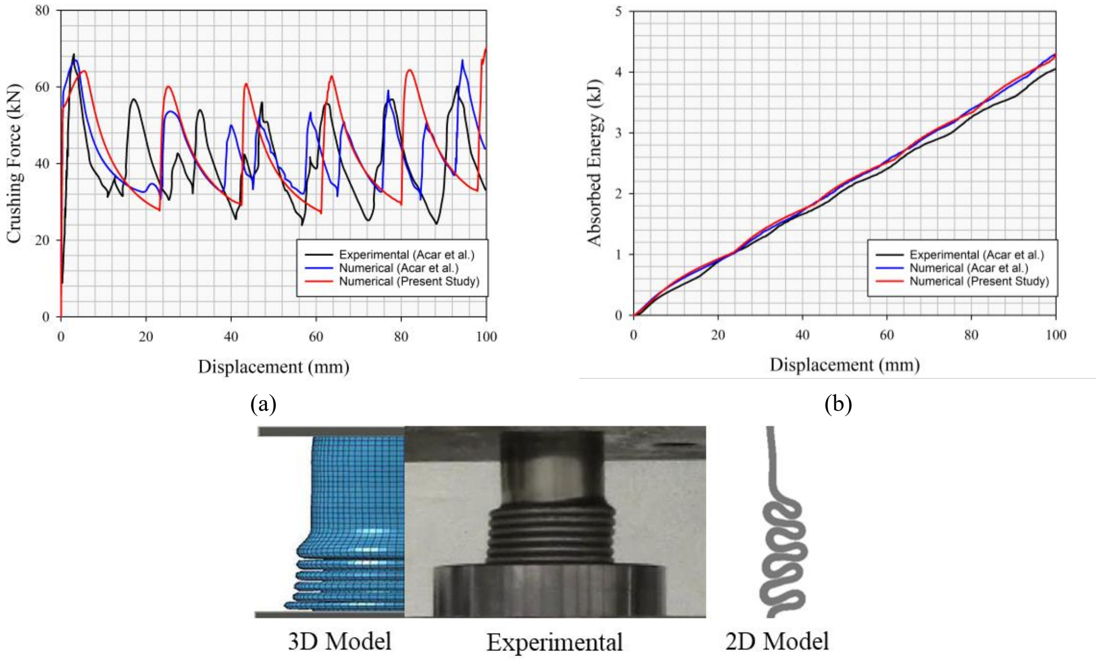

(c)

Fig. 4. The comparison of obtained a) force-displacement, b) absorbed total energy-displacement, and c) deformation images of circular aluminum tube for validation of 2D axially symmetric numerical model

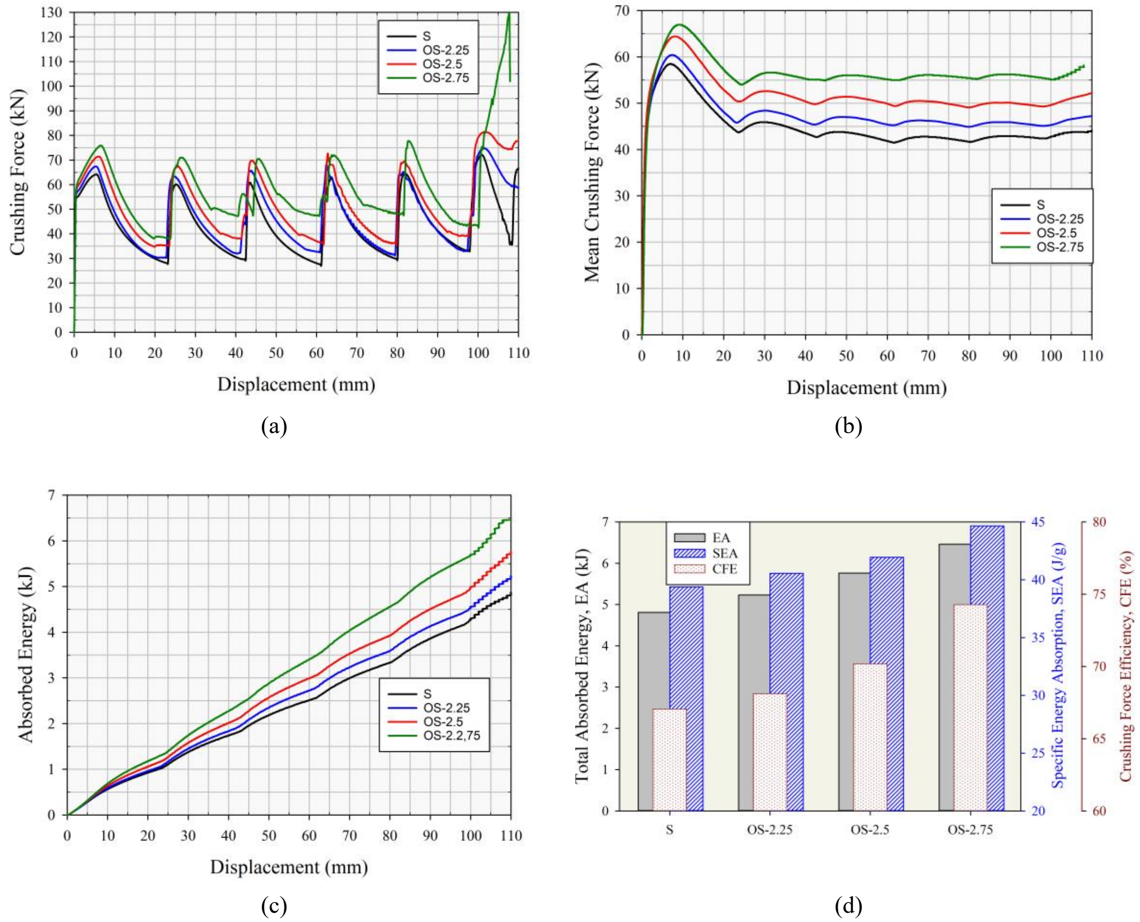

Fig. 5. (a) Crushing force-displacement curves, (b) mean crushing force-displacement curves, (c) absorbed total energy-displacement curves, and (d) crushing performance parameter values obtained from straight and one-sided corrugated tubes

Table 3. The crushing performance parameters for straight, one side and double side corrugated tubes

Specimen	Mass (g)	EA (kJ)	SEA (J/g)	IPF (kN)	MCF (kN)	CFE (%)
S	122.144	4.81	39.4	64.2	42.9	66.8
OS-2.25	128.981	5.23	40.6	67.4	45.9	68.1
OS-2.5	137.337	5.73	41.7	71.5	50.1	70.1
OS-2.75	144.668	6.46	44.7	75.9	56.2	74.0
DS-2.25	128.681	5.35	41.6	67.9	46.8	68.9
DS-2.5	136.635	5.74	42	72.1	50.6	70.2
DS-2.75	140.697	5.77	41.0	74.8	53.2	71.1

From Figs. 5a and 5b and Table 3, it can be observed that the lowest initial peak force was obtained in the straight tube, whereas the corrugated regions with increasing wall-thickness variation resulted in a progressive increase in the initial peak force. For instance, while the initial peak force of the straight tube was approximately 64.2 kN, the corresponding values for the OS-2.25, OS-2.5, and OS-2.75 tubes were 67.4 kN, 71.5 kN, and 75.9 kN, respectively. This corresponds to increases of approximately 5%, 11.4%, and

18.2% with respect to the circular thin-walled tube (S). Similar to the observations reported in the literature, as axial compression begins, the corrugated region undergoes earlier fold initiation, and the increased local wall thickness enhances bending resistance, thereby leading to higher initial peak forces [14].

Similarly, the mean crushing force, which is closely associated with the total absorbed energy over the deformation distance, exhibited increases of approximately 7%, 16.8%, and 31% for the OS-2.25, OS-2.5, and OS-2.75 tubes, respectively, compared to the straight tube. This demonstrates that the sinusoidal-pattern-induced thickness variation in the corrugated zones leads to a significant enhancement in mean crushing force. During deformation, OS tubes tend to generate asymmetric but stable folding sequences, in which the thickened corrugation lobes compact and overlap. This compaction mechanism increases the number of active plastic hinges, which directly increases mean crushing force (MCF) [29]. Consequently, the total absorbed energy also improved as the wall-thickness variation increased. As shown in Fig. 5c and Table 3, the total absorbed energy at a deformation of 110 mm was 4.81 kJ for the straight tube, whereas the OS-2.25, OS-2.5, and OS-2.75 tubes absorbed 5.23 kJ, 5.73 kJ, and 6.46 kJ, respectively.

Another key parameter for evaluating the crushing performance of energy-absorbing elements is the specific energy absorption (SEA). When the absorbed energy per unit mass is considered (Fig. 5d and Table 3), the SEA value of the straight tube was 39.4 J/g, while those of the OS-2.25, OS-2.5, and OS-2.75 tubes increased by 3%, 6%, and 13.5%, reaching 40.6 J/g, 41.7 J/g, and 44.7 J/g, respectively. Despite the slight increase in mass caused by the corrugation with thickness variations, achieving such considerable improvements in SEA highlights the effectiveness of this approach for designing lightweight energy-absorbing structures. A similar enhancement trend is also evident for the crushing force efficiency (CFE), as illustrated in Fig. 5d and Table 3. Overall, the OS designs in the present study exhibit higher SEA and CFE because the thicker corrugation crests act as controlled hinge-formation zones, concentrating plastic deformation and delaying global instability [14].

3.3. Double-sided corrugated tubes

This section shows the effects of double-sided corrugation with variable thickness on the quasi-static compression behavior of a thin-walled tube. The comparison of the crushing force-displacement and mean crushing force-displacement curves obtained from the straight, DS-2.25, DS-2.5, and DS-2.75 tube designs is shown in Figs. 6a and 6b, respectively. Also, obtained crushing performance parameters such as absorbed total energy, initial and mean crushing force values, specific energy absorption capacities, and crushing force efficiency are given in Table 3.

As seen from Figs. 6a and 6b, similar to the one-sided corrugation designs, the initial peak forces for the double-sided corrugated tubes increased with increasing wall-thickness in the corrugation regions. For example, while the initial peak force for the straight tube was 64.2 kN, the corresponding values for the DS-2.25, DS-2.5, and DS-2.75 tubes were 67.9 kN, 72.1 kN, and 74.8 kN, respectively. In addition, the mean crushing force exhibited notable improvements compared to the straight tube, increasing by approximately 9.1%, 17.9%, and 24% for the DS-2.25, DS-2.5, and DS-2.75 tubes, respectively (Table 3).

In terms of the total absorbed energy, as presented in Fig. 6c and Table 3, the DS-2.25, DS-2.5, and DS-2.75 tubes absorbed 5.35 kJ, 5.74 kJ, and 5.77 kJ, respectively. When compared to the straight tube, these correspond to increases of approximately 11.2%, 19.3%, and 20%, indicating a significant enhancement in energy-absorption capability due to the implementation of double-side corrugation with increasing wall-thickness variation. Because both sides are corrugated with thickness variations, DS tubes generally exhibit higher local confinement, which limits excessive radial expansion and results in a more constrained folding mode. This confinement increases the plastic work per unit fold, thereby enhancing absorbed energy, consistent with reports on symmetric corrugation designs [30].

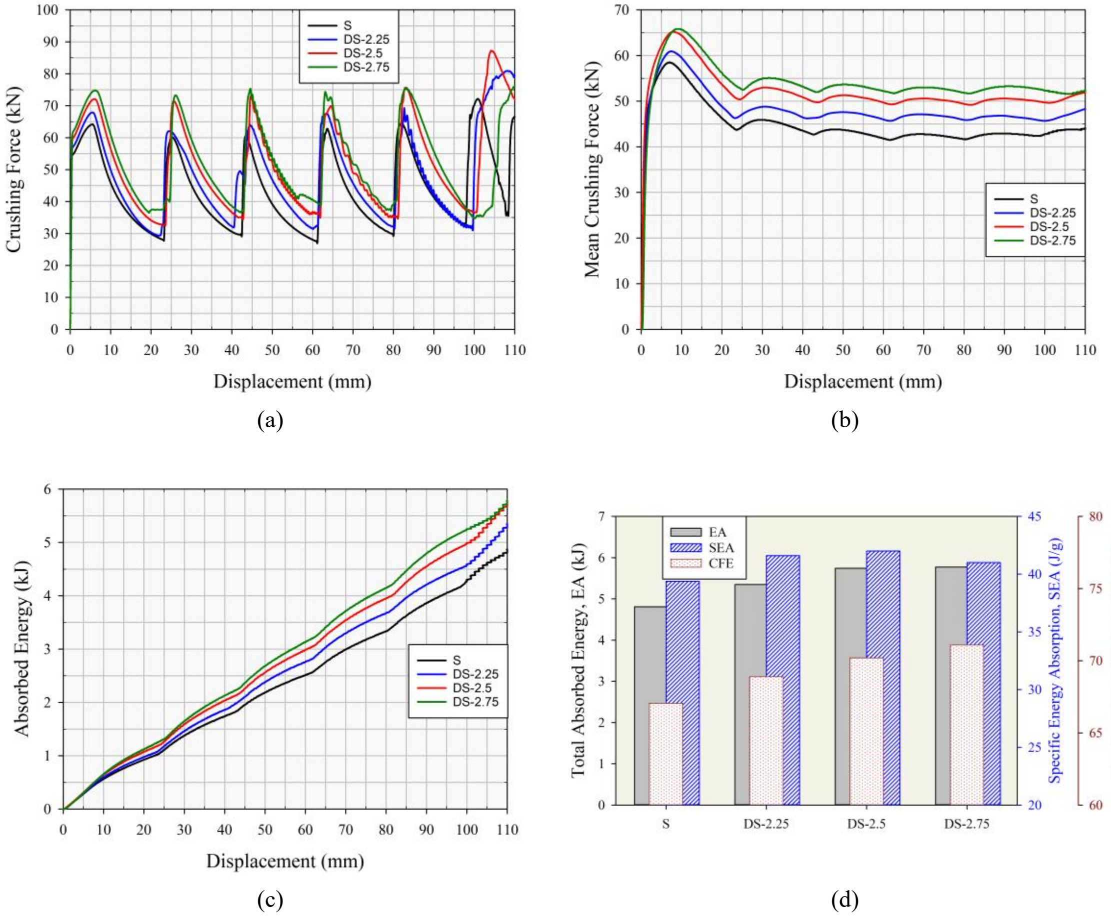

Fig. 6. (a) Crushing force-displacement curves, (b) mean crushing force-displacement curves, (c) absorbed total energy-displacement curves, and (d) crushing performance parameter values obtained from straight and double side corrugated tubes

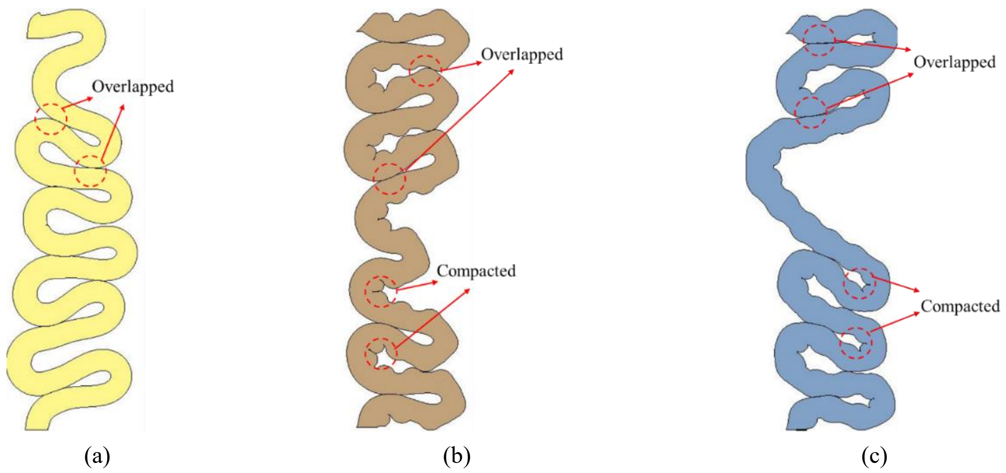

Fig. 7. Deformed shape of the tubes at the end of 100 mm deformation distance obtained from 2D numerical model; (a) straight, (b) OS-2.5, and (c) DS-2.5

To more clearly demonstrate the influence of wall-thickness variation on the energy-absorption performance of the one-sided and double-sided corrugation designs, the obtained SEA values were evaluated (Table 3). For the DS-2.25, DS-2.5, and DS-2.75 tubes, the SEA values were 41.6 J/g, 42.0 J/g, and 41.0 J/g, respectively. Although the SEA values for the double-sided corrugated tubes showed improvements compared to the straight tube, the results indicate that increasing the wall thickness in the corrugation regions does not significantly influence the SEA performance in the double-sided configuration. For example, while the OS-2.75 tube exhibited a 13.5% improvement in SEA relative to the straight tube, the SEA enhancements for the DS-2.5 and DS-2.75 tubes were comparatively modest at 6.6% and 4.1%, respectively.

In terms of overall crushing performance, the OS-2.75 tube demonstrated the highest SEA and CFE values among the one-sided and double-sided designs with variable wall thickness. In addition, it was observed that the OS-2.5 and DS-2.5 tubes exhibited comparable and competitive performance characteristics. For instance, the DS-2.5 tube was slightly lighter than the OS-2.5 tube while offering higher energy-absorption capacity and crush force efficiency. These findings highlight that introducing localized thickness variations within the corrugation regions is an effective design strategy for enhancing the energy-absorption performance of thin-walled tubes and that the corrugation configuration plays a critical role in balancing structural efficiency and crushing capability. This enhancement is primarily attributed to the wall-thickness transitions formed within the corrugated regions exceeding the straight tube thickness, which leads to localized cumulation of deformation and strain. In these thickened zones, the deformation lobes are compacted and overlap during axial crushing, causing the plastic hinges to accumulate and intensify within confined regions. As a result, the local stiffness and bending resistance increase affect the deformation sequence of corrugated tubes. This mechanism enhances strain localization capacity while simultaneously increasing the resistance to plastic hinge formation, thereby generating significantly higher mean crushing forces throughout the deformation process [13, 14, 29]. Consequently, the observed improvement in energy-absorption capability can be attributed to the synergistic effects of localized geometric stiffening and effective compaction in the corrugated and thickened regions. This phenomenon can be clearly observed from the deformed configurations of the S, OS-2.5, and DS-2.5 tubes at a deformation distance of 110 mm, as presented in Figs. 7a-7c.

4. Conclusion

In this study, the axial crushing behavior of circular thin-walled tubes incorporating sinusoidal corrugation patterns with variable wall thicknesses was investigated through 2D axisymmetric numerical modeling. Model validation against both experimental data and 3D finite element results from the literature confirmed the accuracy of the present approach in predicting peak force, absorbed energy, and deformation modes. The findings clearly demonstrate that introducing corrugation-induced thickness variation significantly improves the crashworthiness of thin-walled tubes. Both one-sided and double-sided corrugated designs exhibited higher mean crushing force, total absorbed energy, specific energy absorption (SEA), and crushing force efficiency (CFE) compared with the straight tube. Among all configurations, the OS-2.75 tube achieved the greatest enhancements, improving SEA, CFE, and absorbed energy by 13.5%, 7.2%, and 34.3%, respectively.

Additionally, the OS-2.5 and DS-2.5 tubes provided competitive performance, with the DS-2.5 design offering slightly improved mass efficiency while maintaining comparable energy absorption and crush-force stability. Overall, the results confirm that corrugation-based thickness tailoring is an effective strategy for enhancing the energy-absorption capacity and crashworthiness of thin-walled tubes. Future research will focus on rate-dependent behavior, experimental validation of optimized designs, computational optimization studies, and extending this approach to more complex geometries and material systems.

Declaration of conflicting interests

The author(s) declared no potential conflicts of interest with respect to the research, authorship, and/or publication of this article.

Funding

No funding was received for this study.

Data availability statement

The data that support the findings of this study are available from the corresponding author upon reasonable request.

References

[1] Patel V, Tiwari G, Dumpala R (2020) Review of the crushing response of collapsible tubular structures. Front Mech Eng 15(3):438–474. https://doi.org/10.1007/s11465-019-0579-1

[2] Baroutaji A, Sajjia M, Olabi AG (2017) On the crashworthiness performance of thin-walled energy absorbers: Recent advances and future developments. Thin-Wall Struct 118:137–163. https://doi.org/10.1016/j.tws.2017.05.018

[3] Gao Q, Liao WH (2021) Energy absorption of thin walled tube filled with gradient auxetic structures-theory and simulation. Int J Mech Sci 201:106475. https://doi.org/10.1016/j.ijmecsci.2021.106475

[4] Sun G, Chen D, Zhu G, Li Q (2022) Lightweight hybrid materials and structures for energy absorption: A state-of-the-art review and outlook. Thin-Wall Struct 172:108760. https://doi.org/10.1016/j.tws.2021.108760

[5] Xie S, Zheng S, Zhang J, Liu Z, Wang H, Zhou H (2024) Study on the crashworthiness of multi-cell thin-walled tubes filled with triply periodic minimal surface lattices. Mech Adv Mater Struct 32(3):307–323. https://doi.org/10.1080/15376494.2024.2345206

[6] Ni XH, Zhang XG, Han D, Zhang Y, Jiang W, Teng XC, Hao J, Ren X (2024) Aluminum foam-filled auxetic double tubular structures: Design and characteristic study. Mech Adv Mater Struct 31(15):3377–3388. https://doi.org/10.1080/15376494.2023.2175397

[7] Asanjarani A, Mahdian A, Dibajian SH (2020) Comparative analysis of energy absorption behavior of tapered and grooved thin-walled tubes with various geometry of the cross section. Mech Adv Mater Struct 27(8):633–644. https://doi.org/10.1080/15376494.2018.1488311

[8] Sun H, Wang J, Shen G, Hu P (2016) Energy absorption of aluminum alloy thin-walled tubes under axial impact. J Mech Sci Technol 30(7):3105–3111. https://doi.org/10.1007/s12206-016-0619-2

[9] San Ha N, Lu G (2020) Thin-walled corrugated structures: A review of crashworthiness designs and energy absorption characteristics. Thin-Wall Struct 157:106995. https://doi.org/10.1016/j.tws.2020.106995

[10] Yao RY, Zhao ZY, Yin GS, Zhang B (2021) Attempt to improve the material utilisation and crashworthiness of grooved tube subjected to axial crushing. Int J Crashworthiness 26(1):77–86. https://doi.org/10.1080/13588265.2019.1687162

[11] Li G, Xu F, Sun G, Li Q (2015) A comparative study on thin-walled structures with functionally graded thickness (FGT) and tapered tubes withstanding oblique impact loading. Int J Impact Eng 77:68–83. https://doi.org/10.1016/j.ijimpeng.2014.11.003

[12] Singace AA, El-Sobky H (1997) Behaviour of axially crushed corrugated tubes. Int J Mech Sci 39(3):249–268. https://doi.org/10.1016/S0020-7403(96)00022-7

[13] Eyvazian A, Habibi MK, Hamouda AM, Hedayati R (2014) Axial crushing behavior and energy absorption efficiency of corrugated tubes. Mater Des 54:1028–1038. https://doi.org/10.1016/j.matdes.2013.09.031

[14] Wu S, Li G, Sun G, Wu X, Li Q (2016) Crashworthiness analysis and optimization of sinusoidal corrugation tube. Thin-Wall Struct 105:121–134. https://doi.org/10.1016/j.tws.2016.03.029

[15] Kılıçaslan C (2015) Numerical crushing analysis of aluminum foam-filled corrugated single- and double-circular tubes subjected to axial impact loading. Thin-Wall Struct 96:82–94. https://doi.org/10.1016/j.tws.2015.08.009

[16] Chen DH, Ozaki S (2009) Numerical study of axially crushed cylindrical tubes with corrugated surface. Thin-Wall Struct 47(11):1387–1396. https://doi.org/10.1016/j.tws.2008.12.008
[17] Hao W, Xie J, Wang F (2017) Theoretical prediction of the progressive buckling and energy absorption of the sinusoidal corrugated tube subjected to axial crushing. Comput Struct 191:12–21. https://doi.org/10.1016/j.compstruc.2017.05.001
[18] Liu Z, Hao W, Xie J, Lu J, Huang R, Wang Z (2015) Axial-impact buckling modes and energy absorption properties of thin-walled corrugated tubes with sinusoidal patterns. Thin-Wall Struct 94:410–423. https://doi.org/10.1016/j.tws.2015.05.002
[19] Koloushani M, Forouzan MR, Niroomand MR (2024) Multi-objective optimization of the design parameters in longitudinal corrugated tubes to improve crashworthiness performance. Aerosp Sci Technol 155:109728. https://doi.org/10.1016/j.ast.2024.109728
[20] Alkhatib SE, Matar MS, Tarlochan F, Laban O, Mohamed AS, Alqwasmi N (2019) Deformation modes and crashworthiness energy absorption of sinusoidally corrugated tubes manufactured by direct metal laser sintering. Eng Struct 201:109838. https://doi.org/10.1016/j.engstruct.2019.109838
[21] Mohd Hanid MH, Sharif S, Ahmad M, Suhaimi MA, Khor CY, Ismail KA (2025) Crashworthiness performance of thin-walled structures towards design configuration in vehicle crash boxes application: A review. Int J Crashworthiness 30(6):1–31. https://doi.org/10.1080/13588265.2025.2492975
[22] Baykasoğlu C, Baykasoğlu A, Çetin MT (2019) A comparative study on crashworthiness of thin-walled tubes with functionally graded thickness under oblique impact loadings. Int J Crashworthiness 24(4). https://doi.org/10.1080/13588265.2018.1478775
[23] Wu S, Zheng G, Sun G, Liu Q, Li G, Li Q (2016) On design of multi-cell thin-wall structures for crashworthiness. Int J Impact Eng 88:102–117. https://doi.org/10.1016/j.ijimpeng.2015.09.003
[24] Acar E, Altin M, Güler MA (2019) Evaluation of various multi-cell design concepts for crashworthiness design of thin-walled aluminum tubes. Thin-Wall Struct 142:227–235. https://doi.org/10.1016/j.tws.2019.05.012
[25] Choirotin I, Choiron MA, Purnowidodo A, Darmadi DB (2025) Crashworthiness analysis and optimization of bi-tubular corrugated thin-walled tube under axial loading. Mech Adv Mater Struct 1–14. https://doi.org/10.1080/15376494.2025.2556266
[26] Fu J, Liu Q, Liufu K, Deng Y, Fang J, Li Q (2019) Design of bionic-bamboo thin-walled structures for energy absorption. Thin-Wall Struct 135:400–413. https://doi.org/10.1016/j.tws.2018.10.003
[27] Xu X, Zhang Y, Wang J, Jiang F, Wang CH (2018) Crashworthiness design of novel hierarchical hexagonal columns. Compos Struct 194:36–48. https://doi.org/10.1016/j.compstruct.2018.03.099
[28] Wu J, Zhang Y, Zhang F, Hou Y, Yan X (2021) A bionic tree-liked fractal structure as energy absorber under axial loading. Eng Struct 245:112914. https://doi.org/10.1016/j.engstruct.2021.112914
[29] Wei Y, Yang Z, Yan H, Guo Y, Wu X, Huang C (2016) Proactive regulation of axial crushing behavior of thin-walled circular tube by gradient grooves. Int J Mech Sci 108:49–60. https://doi.org/10.1016/j.ijmecsci.2016.01.033
[30] Mozafari H, Lin S, Tsui GC, Gu L (2018) Controllable energy absorption of double sided corrugated tubes under axial crushing. Compos Part B Eng 134:9–17. https://doi.org/10.1016/j.compositesb.2017.09.042